Agricultural and Forest Meteorology 316 (2022) 108846

Contents lists available at ScienceDirect

Agricultural and Forest Meteorology

journal homepage: www.elsevier.com/locate/agrformet

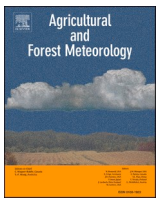

Influence of tree coverage and micro-topography on the thermal environment within and beyond a green space

Zhifeng Wu [a], Wang Man [b], Yin Ren [a,*]

[a] Key Laboratory of Urban Environment and Health, Fujian Key Laboratory of Watershed Ecology, Key Laboratory of Urban Metabolism of Xiamen, Institute of Urban Environment, Chinese Academy of Sciences, Xiamen 361021, China
[b] Department of Spatial Information Science and Engineering, Xiamen University of Technology, Xiamen 361024, China

ARTICLE INFO

Keywords:
Leaf area
Micro-climate modeling
Micro-topography
Thermal environment
Tree coverage
Urban planning

ABSTRACT

The tree coverage of a green space strongly influences its cooling effects; however, knowledge about how the cooling capacity extends beyond a given green space remains limited, along with how modifications to micro-topography affect local thermal environments. Here, we aimed to clarify the cooling effects within and beyond a green space by systematically evaluating differing tree coverage and micro-topographic conditions. Specifically, idealized scenarios were designed and simulated using the micro-climate model ENVI-met. We found that both canopy size and tree number clearly influenced thermal environment conditions within and outside a green space during the daytime. The cooling capacity of the green space during the daytime was linearly correlated with the total leaf area of trees. We also found that modifications to micro-topography had stronger cooling effects on both the green space and adjacent open space in contrast to flat terrain scenarios. Increasing the connectivity of impervious spaces and green areas, along with appropriate micro-topographic modifications, could prevent surrounding impervious surfaces from becoming micro-scale heat islands during the daytime; thus, ameliorating heat stress conditions. The results of this research provide a baseline for climate-adaptive designs and planning of thermally comfortable urban landscapes in the future.

1. Introduction

Heat waves are projected to increase in number, duration, and frequency (Meehl and Tebaldi, 2004). Consequently, urban areas with higher population densities are at greater risk of heat wave-associated morbidity and mortality. The risks of heat wave in urban areas are further amplified by the urban heat island (UHI) effect (Patz et al., 2005). Elevated temperature creates uncomfortable thermal environments, raises energy consumption (to stay cool), and causes air pollution (Battaglia et al., 2017; Ding et al., 2018; Wong et al., 2017; Yadav et al., 2017). Apart from the potential harm of rising temperature to the living environment of humans, it could also be detrimental to the biodiversity of urban species and the integrity of local ecosystems (Merckx et al., 2018).

Urban green spaces supply multiple ecosystem services, and have long been recognized as a potential source of meeting the needs of human livability and biological conservation, leading to increased research interest (Wang et al., 2018). Temperature regulation is an important ecosystem service for increasing the resilience of urban residents to climate change. Many studies have investigated the cooling potential of urban green spaces from various perspectives, including the spatial composition and configuration of green spaces, vegetation type and species, and the interaction between vegetation and the built environment. The percentage cover of vegetation is negatively correlated with temperature (surface temperature and ambient air temperature); consequently, locations with a greater proportional coverage of green space have cooler thermal environments (Kong et al., 2014; Thom et al., 2016; Vaz Monteiro et al., 2016). The spatial configuration is also significantly correlated to the cooling capability of specific green spaces. For example, fragmented green spaces provide effective cooling; however, increased patch density reduces the cooling capacity for fixed amounts of vegetation cover (Kong et al., 2014). The cooling potential of the configuration also depends on vegetation type (Sodoudi et al., 2018). Wu and Chen (2017) showed that the cooling capacity of green space is influenced by the shading of surrounding buildings; thus, optimizing the spatial arrangement of trees in built environments increases the cooling potential of the same amount of green space (Wu and Chen, 2017). Therefore, the cooling capacity within urban green spaces is mainly

* Corresponding author.
E-mail address: yren@iue.ac.cn (Y. Ren).

https://doi.org/10.1016/j.agrformet.2022.108846
Received 10 August 2021; Received in revised form 22 January 2022; Accepted 23 January 2022
Available online 7 February 2022

determined by the process of evapotranspiration and the shading effects of trees. Consequently, several studies have begun exploring these two parameters in relation to the characteristics of green spaces.

Besides the cooling effects within a given green space, the cooling service that it provides extends beyond its boundaries, to cool the immediate environment (Vaz Monteiro et al., 2016). For example, a park of 5 km^2 in Mexico City extended its cooling effect to approximately the width of the park (2 km) (Jauregui, 1990). For small parks (width 20∼60 m) in Tel-Aviv (Israel), the cooling effect was perceived at about 2∼4 times the width of the parks (Shashua-Bara and Hoffman, 2000). With limited space being available in developed urban areas for greening, a frequently asked question is how to maximize the cooling extent of green spaces with fixed areas. The intensity of cooling and the distance over which cooling extends depend on the size of green spaces. Other characteristics of green spaces, such as the vegetation type and canopy structure, also influence the extent of the cooling effect (Potchter et al., 2006). However, the mechanisms that drive the cooling effects of green spaces require clarifying (Vaz Monteiro et al., 2016). Information on the relationship between the cooling capacities a specific green space located in inner urban areas and the outskirts is needed.

Topography also has a substantial impact on the temperature dynamics of urban areas. A previous study showed that both vertical and horizontal temperatures are influenced by micro-topography at small scales. Micro-topography influences the local wind environment and, hence, the thermal comfort levels outdoors. Wind flow across micro-topographic features is quite complicated. Both wind direction and velocity vary greatly around such features (Kondo et al., 2002). Thus, differences in micro-topography and land cover apparently affect spatial-temporal temperature perturbations (Pfister et al., 2017). However, most studies on temperature regulation and cooling extent of urban green spaces were conducted on flat terrain. Assessments and comparisons of thermal effects on the outdoor urban environment in relation to different micro-topographic characteristics are required.

Comprehensively quantifying the variation of local thermal environment requires that one integrate field surveys and numerical modeling to identify the key influential factors. The current study aimed to characterize the spatial-temporal patterns in the near-surface temperature and flow dynamics, and quantify their responses to the tree coverage and micro-topography. To explore subtle changes in near-surface temperatures resulted from micro-topography, surface data need to be collected at a high spatial resolution to reveal the micro-topography, atmospheric structure and dynamic processes near surface, which the commonly used networks of point measurements lack. In present study, a high spatial-temporal resolution numerical model (ENVI-met) was applied to determine how tree coverage and micro-topography influence the cooling extent of a green space of a certain size. ENVI-met is one of the most commonly used numerical model in analyzing the influence of building morphology and vegetation layout on local thermal environment. In order to ensure the reliability of the model's outputs, a calibration is usually carried out by comparing measured values with simulated data. Multiple statistics can be used to evaluate the accuracy of the numerical model. An overview of previous evaluation studies using Root Mean Square Error (RMSE)and index of agreement (*d*) is depicted in Table S1. Factors that affect the accuracy of this model has already been discussed in the past. For example, Yang et al. (2013) indicated that ENVI-met V4 showed better model performance for RMSE and *d* than the previous version based on studies to assess this model. Thus, only a brief discussion of influence from climatic condition and Land Use/Land Cover (LULC) is carried out here. Residential area and university campus are two most common land use types for thermal environment simulation. No universal tendency of the model behavior can be detected among different LULCs. It is not easy to conclude from the collected researches that the LULC exert significant influence over the accuracy of this model. The local climate appears to have an obvious influence on the accuracy of ENVI-met estimation. In three studies which were conducted in Phoenix, USA, Singapore, and Wuhan, China, the model had been used in the same study site for different seasons. The results showed that model performed better in summer season in contrast with other seasons (Hedquist and Brazel, 2014; Roth and Lim, 2017; Zhang et al., 2018). However, in the study of Acero and Arrizabalaga (2018), simulations were conducted based on measured data of three consecutive days with no significant changes in climatic conditions, RMSE and *d* values showed obvious fluctuations (1.00–2.07, 0.83–0.94, respectively). The number of studies collected here was too small to draw firm conclusions. More researches focusing on factors that affect the accuracy of this model are required in the future study. In the present study, the model reliability was first validated by field measurements. Then, we developed and simulated different scenarios of tree coverage (canopy size and tree number) and micro-topography. The results of this study are expected to improve our theoretical and empirical understanding of the underlying mechanism of the cooling effects and extent of green space required in urban areas.

2. Methodology

2.1. Study area

This study was conducted to assess the combined effects of tree coverage and micro-topography based on meteorological conditions and current status of thermal environment in Beijing (39° 28′ N∼41° 05′ N, 115° 25′ E∼117° 30′ E), China. Beijing has undergone rapid urbanization in past four decades. The population has also been increasing as a result of mass immigration. Significant UHI effects have been identified over the inner-city areas, by comparing near-surface air temperatures between urban and rural areas based on meteorological measurements (Wang et al., 2009; Zheng et al., 2018). Increasing vegetation, especially trees, is regarded as an effective strategy to ameliorate the deleterious effects of UHI (Akbari and Kolokotsa, 2016; Lee et al., 2016). The municipal government of Beijing has implemented the green growth strategy since 1978, with urban green coverage increasing from 22.3% in 1978 to 48.4% in 2018 (Beijing Statistics Bureau, 2019); however, Beijing's urban thermal environment continues to degrade (Ge et al., 2016). Our study targeted the densely urbanized inner-city area, with elevation varying from 20 to 60 m above sea level. Hundreds of green space patches are scattered throughout the area, ranging from 680 ha (Olympic Forest Park) to less than 0.01 ha (roadside green spaces). Investigating how to maximize the cooling capacity and extent of existing green spaces is beneficial to the wellbeing of the urban citizens living within and beyond this area.

2.2. Numerical model of micro-climate

2.2.1. On-site measures of micro-climate

Field measurements of local weather conditions were conducted at two sites in Beijing city, including the Wang-Chun-Yuan residential quarter and the Beijing Olympic Forest Park. The monitoring of meteorological factors conducted in the Wang-Chun-Yuan residential quarter continued from August 10th to 18th, 2014. This period was selected to obtain various climatic data for typical summer days. A portable weather station (Onset HOBO U30) was placed in an open space at the center of a pocket park in Wang-Chun-Yuan residential quarter with> 10 m away from surrounding trees and buildings. HOBO U30 weather station is a weatherproof data logger designed for environmental monitoring applications. This logger has a built-in rechargeable battery and supports up to 10 plug-and-play smart sensors. Four sensors including solar radiation sensor, temperature sensor, relative humidity sensor, wind speed/direction sensor were used in this study. The solar radiation sensor is a light sensor (silicon pyranometer) with a measurement range of 0 to 1280 W/m^2. The accuracy and resolution of this sensor are ±10 W/m^2 and 1.25 W/m^2, respectively. The temperature sensor has a measurement range of −40 to 75℃ (accuracy: ±0.21℃ from 10 to 50℃, resolution: 0.02℃). The relative humidity sensor has a

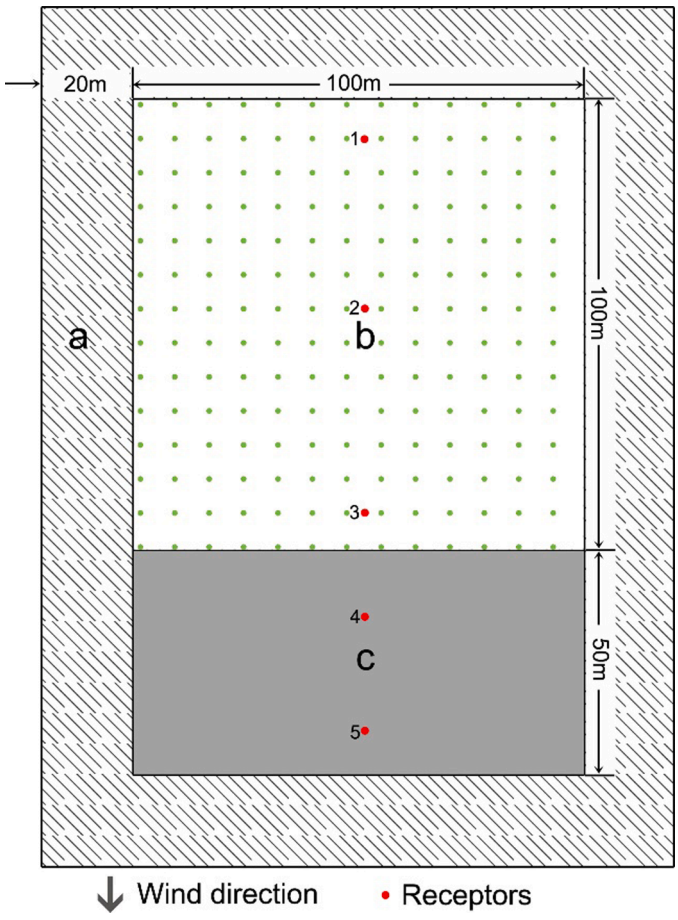

Fig. 1. Configuration of an ideal landscape. a: nesting border, b: green space, which is the model domain for tree arrangements and micro-topographies, c: open space, which is the model domain for estimating how far the cooling effect extended from the green space;1 5: receptors.

measurement range of 0–100% (accuracy: ±2.5% from 10 to 90%, resolution: 0.1%). The wind speed smart sensor can record wind speed from 0 to 45 m/s (accuracy: ±1.1 m/s, resolution: 0.5 m/s). Six temperature/relative humidity data loggers (HOBO pro v2, accuracy: ±0.2℃, resolution:0.02℃) were mounted on tree trunks or electrical poles at the height of 2 m. The field measurement of meteorological factors of the Beijing Olympic Forest Park was conducted from July 5th to July 9th, 2020. Two temperature and relative humidity data loggers were mounted on tree trunks in forest on flat terrain, and forest of a small hill (< 50 m). Other two loggers were mounted on electrical poles of roadside and water side. All these meteorological factors were recorded at a frequency of 1 min. Recorded meteorological data of two days with no precipitation (August 14th, 2014 and July 7th, 2020) were used to verify the simulated results of the micro-scale climate model.

2.2.2. Model selection

ENVI-met is a three-dimensional micro-climate model that was selected to simulate variation in the thermal environment. ENVI-met facilitates analyses of high spatial-temporal resolution, comprehensively integrating all the key processes, including evapotranspiration, shading, and ventilation. Consequently, it is highly suitable for use in evaluating micro-climate changes resulting from landscape modification (Sodoudi et al., 2018). ENVI-met has been widely used in studies of micro-climate globally. It has been tested and validated for various land use types and climatic regions (Emmanuel and Loconsole, 2015; Ghaffarianhoseini et al., 2015; Herath et al., 2018; Kong et al., 2016; Simon et al., 2018). The core model of ENVI-met encompasses three sub-models. Each sub-model was designed to address specific processes related to thermal balance. The atmospheric sub-model is mainly based on the fundamental laws of computational fluid dynamics. It predicts the evolution of air movement, including wind direction and velocity, air temperature and humidity, and air turbulence. Calculations of the absorption and emission of short- and long-wave radiation are also included in this sub-model. The vegetation sub-model addresses all of the ecological processes related to vegetation system (Wu and Chen, 2017). In this model, vegetation is not just a physical obstacle against wind and radiation, but is also a biological body that interacts with the surrounding environment by exchanging heat and water vapor (Ali--Toudert, 2005; Simon, 2016). The atmospheric and vegetation sub-models were used to obtain a quantitative estimate of the cooling capacity and extent of green space. ENVI-met produces multiple meteorological parameters and thermal comfort parameters. In addition, ENVI-met allows the end-users to examine each outputted parameter from a three-dimensional perspective, making the extremely complex heat balance process more intuitive for interpretation. In the present study, ENVI-met 4.4.3 was employed to explore the influence of tree coverage and micro-topography on local thermal environment.

2.2.3. Simulation preparation

The ENVI-met model consists of a three-dimensional core model which is encapsulated within a one-dimensional model. The 3D core model includes all atmosphere, soil, building and vegetation processes and the 1D model provides the boundary conditions that are required for the lateral and vertical borders of the 3D model (Simon, 2016). Multiple independent input data, such as latitude, longitude, the date and duration of the simulation, the horizontal wind speed at 10 m' height, the roughness length, the air temperature in 2 m' height, and the relative humidity in 2 m' height are required to create the vertical profiles of the 1D boundary model. In the present study, an ideal landscape was designed in the 3D model to evaluate the cooling capacity and cooling extent of a green space. The whole domain of the ideal landscape was 1.5 ha (100m × 150 m), with 1.0 ha as greenspace for tree arrangement and micro-topographic modification and the other 0.5 ha as open space to evaluate the cooling effect extending from upwind of the green space

Table 1
Configuration data of the simulation.

Parameter	Item	Value/ Name
Simulation time	- (h)	16
Meteorological conditions	Wind speed measured in 10 m height (m/s)	2
	Wind direction (0: N, 90: E, 180: S, 270: W)	0
	Minimum air temperature at 2 m (℃)	20
	Maximum air temperature at 2 m (℃)	31.9
	Minimum relative humidity (%)	40.7
	Maximum relative humidity (%)	83.7
Profile types	Soil profile for green space	Loamy soil
	Soil profile for open space	Asphalt
	Soil profile for nesting grids	Loamy soil
Loamy soil data	Initial temperature upper layer (0–20 cm) (℃)	24.85
	middle layer (20–50 cm) (℃)	22.85
	deep layer (below 50 cm) (℃)	20.85
	Relative humidity upper layer (0–20 cm) (%)	15
	middle layer (20–50 cm) (%)	19
	deep layer (below 50 cm) (%)	21
	Roughness length (m)	0.015
	Albedo	0.000
	Emissivity	0.980
Asphalt data	Volumetric heat capacity ($J/m^3K \times 10^{-6}$)	2.214
	Heat conductivity (W/(m•K))	1.16
	Roughness length (m)	0.010
	Albedo	0.200
	Emissivity	0.900

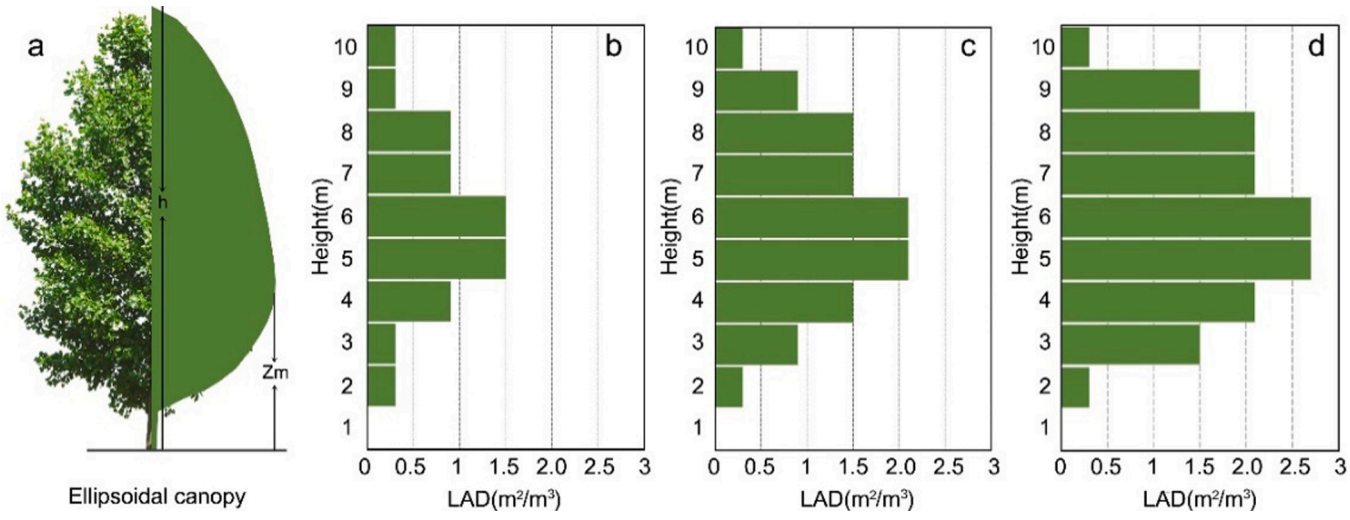

Fig. 2. LADs of the three scenarios for canopy size. a: ellipsoidal tree canopy; b: smallest canopy size sub-scenario (S1); c: medium canopy size sub-scenario (S2); largest canopy size sub-scenario (S3).

(Fig. 1). The model domain was built with 50 × 75 × 30 three-dimensional cells, with each cell having dimensions of 2 × 2 × 3 m. In addition, we added a 20-grid-deep border to the perimeter of the model to enhance stability when simulating elements were located close to the border of the main model domain. ENVI-met 4.4.3 allows users to employ the measured local weather data as inputs by forcing the model to follow user's inputs during the simulation. In this study, simple forcing of lateral boundary conditions was adopted to initialize the simulation. Hourly averaged air temperature and relative humidity at 2 m, wind speed and direction at 10 m, and global radiation values were based on field measurements made over days at two locations, and these data were used to parameterize the 1D boundary model. Cloud cover conditions were used in the forcing of solar radiation. The algorithm (Eq. (1)) is implemented in this study to calculated the cloud cover (Kasten and Czeplak, 1980):

$$\frac{G(N)}{G(0)} = 1 - 0.75\left(\frac{N}{8}\right)^{3.4} \tag{1}$$

where N is the number of eights of the sky obscured by clouds; G(N) is the global radiation at total cloud amount N okta; G(0) is the global radiation at cloudless sky.

The simulation lasted 16 h from 07:00 to 22:00. Based on the meteorological conditions of study area and the designed scenarios, the configuration file of the designed scenario is shown in Table 1. The roughness length, albedo, and emissivity of profiles were kept at default values of ENVI-met database. Receptors are selected points inside the ENVI-met model area, where processes in the atmosphere and the soil are monitored in detail. In this study, three receptors (1, 2 and 3) were set to record the near-surface temperature variations of the greenspace (b), two other receptors (4 and 5) were set to record the temperature variations of the open space. Then, cooling capacity was calculated by comparing the average values of temperatures of receptors 1, 2, 3 and 4, 5 (Eq. (2)).

$$\text{Cooling capacity} = Average\left(\sum_{1}^{3} Ta\_receptor_j\right) - Average\left(\sum_{4}^{5} Ta\_receptor_j\right) \tag{2}$$

where *Ta_receptor* is the air temperature at the height of 2 m above ground.

2.3. Development of the scenario

Two tree coverage scenarios (canopy size and tree number) and micro-topography scenario were designed in the SPACES module of ENVI-met. The influence of wind speed on the cooling effect of green space was also evaluated.

2.3.1. Canopy size scenario (Flat terrain)

In ENVI-met, the leaf area density (LAD) is an important variable related to multiple processes, including solar interception, evapotranspiration, wind dragging, and additional atmospheric turbulence, due to vegetation. LAD determines the size of the plant-atmospheric interface, contributing to the exchange of energy and mass between vegetation and atmosphere (Jonckheere et al., 2004). We first measured the LAIs using a LAI-2000 plant canopy analyzer for major tree species, including *Acer mono Maxim, Firmiana simplex, Sophora japonica, Pinus tabulaeformis, Juniperus chinensis, Platycladus orientalis*, which are amongst the most widespread tree species planted in residential quarters and urban parks in Beijing (Zhao, 2010). Then the LADs of *Acer mono Maxim* was calculated according to the empirical LAD model (Lalic and Mihailovic, 2004) to develop tree models with different canopy sizes and LADs. The calculation of LAD with Eqs. (3) and ((4):

$$LAI = \int_0^h LAD(z)dz = \int_0^h L_m\left(\frac{h - z_m}{h - z}\right)^n \exp\left[n\left(1 - \frac{h - z_m}{h - z}\right)\right]dz \tag{3}$$

$$n = \begin{cases} 6\ 0 \le z < z_m \\ 0.5\ z_m \le z \le h \end{cases} \tag{4}$$

where h is tree height, L_m is the maximum value of LAD at the corresponding height of z_m, z is the height of different layers of tree canopy, and n is the number of the layers. Then, the calculated LADs were put in

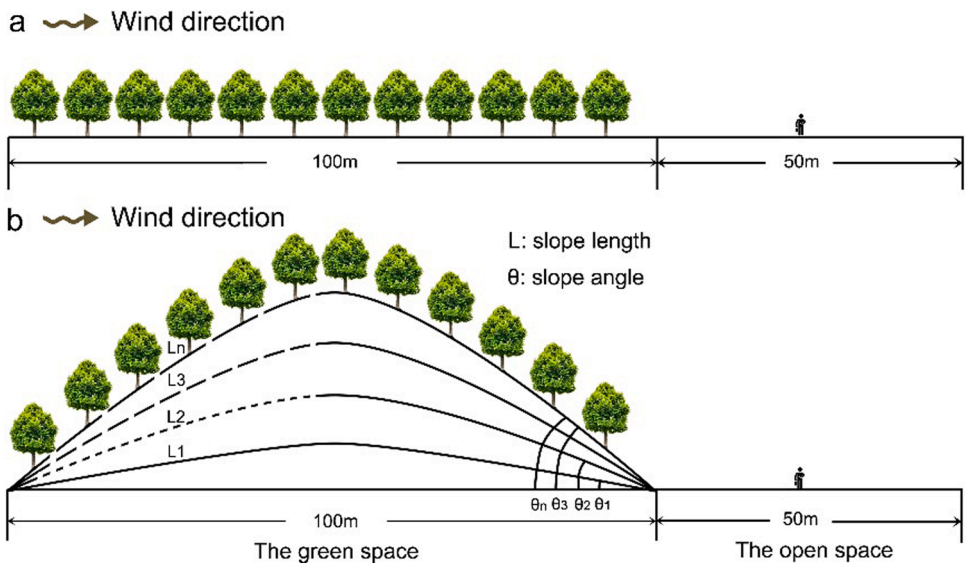

Fig. 3. Schematic of the micro-topography scenarios. a: flat terrain with trees, b: micro-topography with different slope lengths and slope angles.

the ENVI-met plant database for 3-D reconstruction of the tree canopy. An ellipsoid shaped tree canopy (Fig. 2a) was selected to develop the three sub-scenarios with different canopy sizes to analyze how the amount of leaf area influences the thermal environment. These three types of canopies had the same height (10 m). The ellipsoid shaped tree canopy (Fig. 2a) served as the smallest canopy size sub-scenario (Fig. 2b, S1). The LADs of all layers, except the top and bottom layers, of S1 were increased by 0.6 to form the medium canopy sub-scenario (Figs. 2c, S2). The LADs of S2 were increased a further 0.6 to form the largest canopy sub-scenario (Figs. 2b, S1). The canopy radius at the maximum value of LAD increased from 5 m in S1 to 7 m in S2 and 9 m in S3. For all three sub-scenarios, 10 × 10 trees were evenly distributed in the green space. The total leaf area of the three canopy size sub-scenarios was 2430 m^2, 5790 m^2, and 10,830 m^2, respectively.

2.3.2. *Tree number sub-scenario (flat terrain)*

Using the same canopy size as S3, three sub-scenarios of different tree numbers were developed. In the lowest (N1), medium (N2), and highest density sub-scenario (N3), there were 7 × 7, 10 × 10, and 12 × 12, ellipsoid canopy trees, respectively, planted in the same green space. The total leaf area of these three scenarios was 5306.7 m^2, 10,830 m^2, and 15,595.2 m^2, respectively. S3 had the same tree arrangement as N2.

2.3.3. *Micro-topography scenario*

An increase in surface roughness leads to an increase in surface area. Among the formative factors of the urban climate, roughness due to buildings and the thermal property of construction materials contribute heavily to the appearance of the UHI phenomenon (Tejima, 1995). Modifying the topography or roughness of the land surface can increase the area for planting more vegetation to mitigate UHI effects. In addition, wind flow around micro-topographic features is rather complicated (Kondo et al., 2002). Wind direction and velocity vary significantly when air flow over these topographies, and wind flow clearly affect micro-climate air temperature. Hence, it is very important to estimate the flow fields around micro-topographies and to reflect them in the mitigation of UHI effect. In this scenario, several sub-scenarios with small hills of different slope angles and lengths were developed. Fig. 3b shows the vertical section of these sub-scenarios. The small hill spread across the landscape, with the direction of the ridge line being perpendicular to the wind direction. To study the effect of wind speed with respect to the variations of micro-topographies, two different wind speed at 10 m above the ground (1 m/s and 3 m/s) were simulated for each of the slope angles and lengths sub-scenarios.

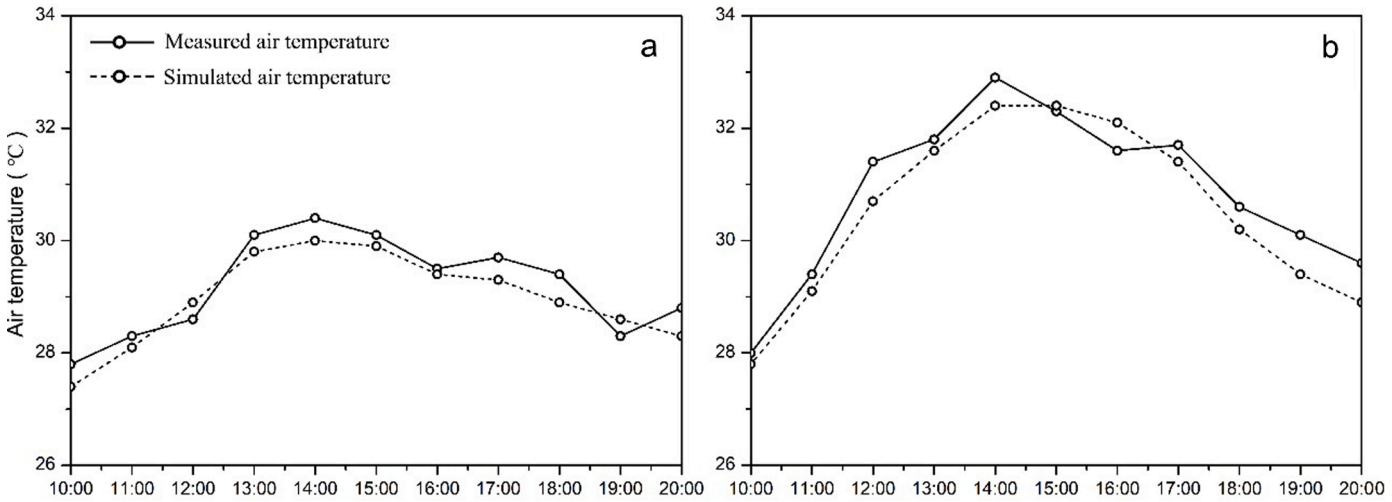

Fig. 4. Comparison between measured and simulated air temperatures. a: July 7th, 2020; b: August 14th, 2014.

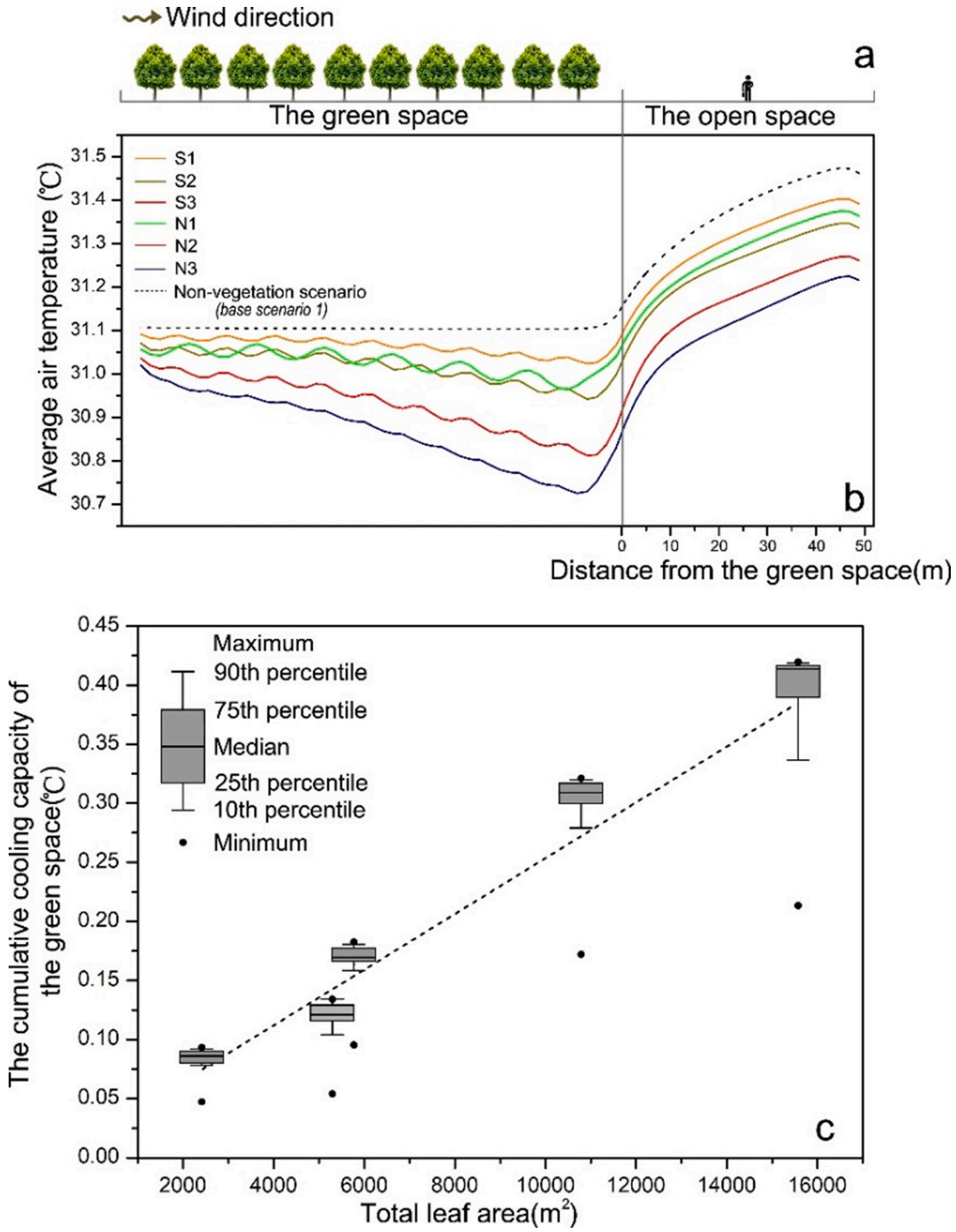

Fig. 5. a: Schematic of landscape composition and wind direction; b: Comparison of near-surface temperature between the non-vegetation scenario with different tree coverage scenarios at 14:00; c: the relationship between total leaf area and cooling capacity.

2.4. Analysis of the simulated data

The air temperatures at 2.0 m above ground level from10:00 to 20:00 were extracted from the simulated results of the sub-scenarios. At 14:00, the outdoor air temperature was highest during the simulated day, and the green space was expected to represent the strongest cooling capacity. It is interesting to analyze how green space performs during this time period, with only outward heat fluxes into atmosphere. First, the canopy size sub-scenarios and the tree number sub-scenarios were compared with the non-vegetation scenario to investigate the cooling effects of different characteristics of green space. Pearson's correlation analysis was conducted between near-surface air temperatures and total leaf area of trees. The statistical analysis was applied with IBM SPSS Statistical 19. Second, one of the tree arrangement sub-scenarios was selected as the second baseline scenario. The simulation results of the slope length sub-scenarios and slope angle sub-scenarios were compared against the second baseline scenario to explore the influence of micro-topography on near-surface temperature.

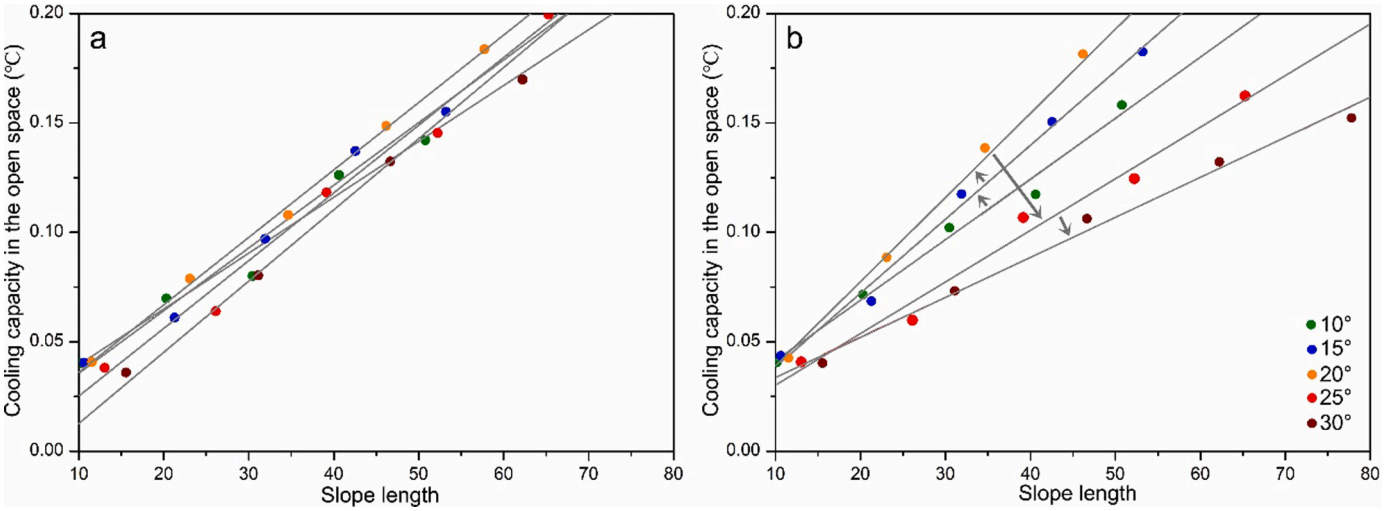

Fig. 6. The relationships between cumulative cooling capacity and slope length and slope angle. a: the wind speed is 1 m/s at 10 m above the ground; b: the wind speed is 3 m/s at 10 m above the ground.

3. Results

3.1. Evaluation of the model results

Ideal scenarios were constructed to investigate how tree coverage and micro-topography influence the cooling effects of a green space, both in it and outside it. Finding such landscapes with similar vegetation patterns and topographic features in reality is difficult. Therefore, we validated the model in a residential quarter that had complex spatial patterns for various landscape components, including buildings, vegetation, small hills, artificial lakes, and open spaces. Also, we conducted a confirmatory simulation in a green space with small-scale topographic relief and various tree canopy coverage of the Beijing Olympic Park. These two models of the Wang-Chun-Yuan residential quarter and the greenspace landscape in the Beijing Olympic Forest Park were built based on high-resolution remote sensing image in SPACES module of ENVI-met. Leaf Area Indices and tree heights of major tree species in these two sites were measured using plant canopy analyzer (LAI-2000) and altimeter, respectively. Three-dimensional cells were built as component of buildings, trees and small hill. The cell had the dimensions of $2 \times 2 \times 3$ m in these two validation models and the other prediction models. Verifications of the two validation models were conducted by comparing near-surface temperatures (2 m above ground) of field measurements and ENVI-met outputs. The Root Mean Square Error (RMSE) and the index of agreement were calculated to evaluate the simulation results accuracy. The measured temperatures were hourly averaged data from HOBO U30 weather station and temperature/relative humidity data loggers. The modeled temperature referred to the mean air temperature at 2 m above ground of the whole Wang-Chun-Yuan residential quarter and the greenspace landscape in the Beijing Olympic Forest Park, respectively (Fig. 4a, b). We assumed that if the simulation results of ENVI-met for the residential quarter and urban park were reliable, the model could produce reliable simulation results under ideal scenarios. The same input parameters as in Fig. 4 were used in the simulation of the residential quarter and urban park.

Even though the measured temperature was generally higher than the predicted temperature throughout most of the day (at 2 m above ground), the model generally showed good agreement with field measurements. The correlation coefficient between simulated temperature and measured temperature at July 7, 2020 was 0.96, RMSE was 0.67 °C, and the index of agreement was 0.93. The corresponding coefficients at August 14, 2014 were 0.95, 0.72 °C, and 0.95, respectively. With the relatively low RMSE and high correlation coefficient, we considered the simulation results of ENVI-met to be reliable. The good performance of a model provides us opportunities to conduct exploratory investigations by setting various ideal scenarios, which can be impracticable in reality. In the present study, analysis of combined influence of vegetation layout and micro-topography on local thermal environment have been carried out based on validation of simulation results. A total of 31 ideal scenarios, including 6 sub-scenarios of tree arrangements on flat terrain and 25 sub-scenarios of tree arrangements on undulating terrain, were designed and simulated. We believe that the modeling results presented in this paper have some value on thermal environment mitigation by greenspace arrangement and micro-topographic modification at neighborhood or block scale. Of course, further studies to support and confirm our results are necessary.

3.2. Effect of tree coverage on near-surface air temperature

Our study area contained two different patches. The green space patch located on the upwind side and the open space patch situated on the downwind side. We first aimed to evaluate how tree coverage affected the local thermal environment. Compared with the non-vegetation scenario (base scenario 1), all tree coverage scenarios, including sub-scenarios with different canopy sizes (S1–S3) and planting densities (N1, N2, and N3), showed various levels of cooling capacity at 14:00 (Fig. 5b). Along the wind direction, the cooling effects of all tree coverage sub-scenarios gradually increased (from 0.02 ℃, 0.04 ℃, 0.05 ℃, 0.07 ℃, and 0.08 ℃ to 0.08 ℃, 0.16 ℃, 0.14 ℃, 0.29 ℃, and 0.38 ℃ for S1, N1, S2, S3/N2, and N3, respectively. When the air moved across the boundary between the green space and the open space, the air temperature for all scenarios, including non-vegetation scenario and tree coverage sub-scenario, clearly declined. The decline in air temperature was mainly caused by changes to the thermophysical properties of the pavement surface layer, which has lower reflectivity and higher solar absorptivity. Air temperature in the open space declined; however, tree coverage sub-scenarios had 0.07 ℃ (S1), 0.10 ℃ (N1), 0.13 ℃ (S2), 0.20 ℃ (S3/N2), and 0.25 ℃ (N3) lower near-surface air temperature compared to the non-vegetation scenario 150 m distance. However, at 20:00, tree coverage sub-scenarios had slightly higher air temperatures compared to the non-vegetation scenario in the green space. No significant differences to air temperature was found in the open space among tree coverage sub-scenarios.

Leaf area significantly influences the cooling capacity of green spaces. Fig. 5c shows the largest near-surface cooling capacity (at 92 m distance) for the tree coverage sub-scenarios. The model results showed a linear relationship between total leaf area and near-surface cooling effects, with $R^2 = 0.98$, and a 0.05 ℃ increase in cooling capacity per

1000 m^2 increase in total leaf area. The air temperature at 14:00 and 20:00 at 92 m distance showed differences in air temperature of 3.85 ℃, 3.79 ℃, 3.76 ℃, 3.61 ℃, and 3.56 ℃ for the non-vegetation scenarios, S1, N1, S2, S3/N2, N3, respectively. Larger leaf area leads to smaller temperature differences between these two time points.

3.3. Effect of micro-topography on near-surface air temperature

The micro-topography had a clear influence on near-surface air temperatures. For all slope angles and lengths sub-scenarios, the near-surface air temperature of the hillside was lower than that of the flat terrain scenario at daytime. The lowest air temperatures of these sub-scenarios occurred on hillsides shielded from the wind, rather than the ridge. Despite having the same tree arrangement, these micro-topography modification sub-scenarios had lower air temperature in the open space scenario compared to the flat terrain scenario. With the increase in slope length, the cumulative cooling capacity at the open space generally showed a growing trend for both two wind speed conditions (Fig. 6). For the combined effects of slope angles and lengths, we found there were no significant differences among the micro-topographic sub-scenarios when the wind speed is relatively low (1 m/s at the height of 10 m above the ground) (Fig. 6b). For relatively higher wind speed condition (3 m/s at 10 m above the ground), however, the modifications from micro-topographic variations on near-surface air temperatures represented a different result. When the slope angle increased from 10° to 20°, the micro-topography modification presented an enhanced cumulative cooling capacity. However, the cooling capacity of the corresponding slope angle sub-scenario has been on a weakening trend as the slope angle continuously increased from 20° to 30° (Fig. 6b).

4. Discussion

4.1. Cooling effects within and beyond the greenspace with different tree coverage and micro-topography

Vegetation represents an important element for mitigating heat, especially during the day time (Smardon, 1988). The importance of tree coverage for mitigating heat has been previously reported (Hamada and Ohta, 2010; Myint et al., 2013), with our research providing further evidence for the cooling mechanisms, by presenting the linear relationship between total leaf area and cooling capacity. The cooling capacity of vegetation mainly depends on two key processes: shading and transpiration (Bowler et al., 2010). The leaf is the main plant organ that directly contributes to both two processes. In the present study, all tree coverage sub-scenarios were effective at cooling the local thermal environment in contrast with the non-vegetation scenario at 14:00. During the daytime, solar radiation is the main contributor to the heat gain of the land surface. Trees affect local air temperature by transpiring water through their leaves and by blocking solar radiation, which reduces the absorption of radiation and heat storage by various anthropogenic surfaces. Trees also alter the wind characteristics that affect air dispersion (Nowak et al., 1998). When air flows through a green space, the thermodynamic properties of air are modified at some level. The cooling effects of vegetation are then transferred to next landscape via moving air. Higher tree density and crown coverage can reduce the speed of the wind moving through the forest canopy and then increase the time for the thermal properties of the air mass to change. As the air mass driven by wind passes through the green space to adjacent open space, it can carry out cooling by a higher cooling capacity in the near-surface thermal environment. Fig. 4b clearly showed that significant temperature changes occurred when air moved between landscapes with different thermophysical properties. When air mass moved further into the open space, the near-surface air temperature continued to increase but at a declining rate. As previously mentioned, we added a 20 nested grid cells to the core domain to minimize boundary effects. The nested area is a band of grid cells surrounding the core domain (including the green space and the open space), which can keep the model boundaries away from the core and thus lower the calculation uncertainties occurring at the boundaries (Kong et al., 2016). In the present study, the nested grid surface was set to a single soil profile (loamy soil) which has lower albedo and higher roughness length and emissivity comparing with the asphalt surface of the open space. The transition of thermophysical properties of soil profiles from the open space to surrounding nesting grids led to a small cooling process at the end of the simulation domain. At night (20:00), the cooling capacity of various tree coverage sub-scenarios markedly decreased, and even disappeared. After sunset, the transpiration rates of various plants, including trees, is usually just 5~15% that of daytime values (Caird et al., 2007). Gradually warmed air during the daytime is trapped within and below tree crowns, due to reduced turbulent exchange with air above the canopy (Zölch et al., 2019). Thus, trees act as a thermal insulation layer for the atmosphere beneath tree crowns, resulting in trees providing cooling effects during the daytime, and non-effect or warming effects at night.

The results showed that there was also a linear relationship between total leaf area and the distance where the cooling effect produced by the upwind direction (r^2=0.97) when the wind speed was set to 1 m/s. The surface topography variation made the relationship between the green space and the distance into the open space where the cooling effect was almost vanished more complicated. The combination of tree coverage and micro-topography can further reduce near-surface air temperature during the daytime. All of the sub-scenarios with different tree coverage and micro-topography cooled down the greenspace and the open space in the downwind direction. Air temperature drops rapidly as the height of the surface increases. However, the decreasing rate of air temperature is not directly proportional to the height of the small hill. It has been shown that there is a relationship between the cooling amplitude of the near-surface atmospheric temperature with the slope length and the slope angle (Fig. 6b). The increase in slope length increases the distance that the air travels through the green space, so more cooling will be accumulated and then passed to the downstream air. The slope angle mainly affects the direction of air flow, and the greater the wind speed, the greater the effect it has on the downstream air properties. When the wind speed gradually increases, the influence of the slope angle on the downstream air temperature change significantly. When the wind speed is 1 m/s, the near-surface air temperature only decreases linearly with the increase of the slope length, and the slope has no obvious effect, but when the wind speed increases to 3 m/s, under the same slope length condition, the cooling effect of near-surface temperature first increases (10° −20°), followed by a rapid fall (20°−30°). Future work should conduct a more detailed analysis of the effect of slope angle on air temperature in the downwind direction to determine the best slope under common wind speed conditions.

4.2. Implications on the planning and management of urban thermal environments

Urban development replaces natural landscapes with artificial impervious surfaces, which often absorb large quantities of incident solar radiation and discharge a fraction of the solar absorption as sensible heat into the near-surface atmosphere. Impervious surface coverage is a key environmental indicator that is closely correlated with the thermal urban environment. In the absence of design measures to mitigate heat, impervious surfaces become micro-scale heat islands, causing severe heat stress (Vanos et al., 2016). In comparison, urban green spaces are cooler than surrounding areas, creating a cool island effect that improves the climatic conditions of urban areas and reduce heat stress produced by heat islands (Hamada and Ohta, 2010). Forest with higher leaf area density can provide a more stable understory thermal environment, that is, air temperature inside of the forest is usually higher than the outside in daytime and lower than the outside at

night. It has been proved by this study that the cooling capacity of the green space in the upwind direction is positively correlated with the total leaf area of the trees. In addition, supporting previous studies, the present study showed that green spaces introduce cold air to surrounding built-up areas. The role of urban green space is not only to improve the thermal environment inside the green space, but to achieve the improvement of the thermal environment of the entire city. Therefore, expanding the scope of single green space's cold island effect and connecting the influence of the surrounding small green spaces to form a greater "cooling island" can be an effective strategy for the improvement of the urban thermal environment.

Micro-topography has a strong impact on spatial-temporal temperature dynamics (Pfister et al., 2017). Remote sensing technology confirmed that topography increases the cooling effect of green spaces located on hills facing surrounding urban areas (Hamada et al., 2013). Complex urban landscape systems are composed of interacting patches with differing thermal properties, with complicated boundaries generating diverse thermal landscapes. Supporting previous studies, the current study showed that the suitable use of topography expands the cooling effect; thus, more strategies could be applied to improve urban micro-climates by using micro-topography to regulate the urban thermal landscape. For example, the combination of vegetation and micro-topography can be used to produce a stronger air cooling effect on a small spatial scale such as residential quarter and pocket park. In this way, the scopes of scattered "cold island" expand. However, of note, micro-topographic scenarios introduce noticeable warming effects on the leeward open space at night. With greater wind speeds, the warming effect extending from the green space to the open space also increases. Consequently, strategies implemented to improve the thermal environment could have contrasting effects at different times of day (Zölch et al., 2019). Therefore, management strategies should decide in advance whether the aim is to mitigate heat during the day, at night, or both to implement the appropriate modifications.

The selection or modification of appropriate micro-topography has long been conducted in the urban and rural areas of China for multiple purposes, including creating comfortable living environments, enhancing security against possible attacks from outsiders, and increasing esthetic value. Modifying the micro-topography of today's cities could generate such positive environmental benefits. For example, the appropriate modification of micro-topography in the construction of urban wetlands could improve their ecological function in water conservation (Liu et al., 2020). To improve the urban thermal environment, micro-topography could be modified in residential areas and parks. Limited land is available, and the expansion of green areas is not practical in major cities, like Beijing metropolis. Thus, urban designers and planners should consider incorporating micro-topography as a potential measure to maximize the cooling effects of limited green spaces.

4.3. Limitations and future directions

The present study applied the ENVI-met 4.4.3 model to simulate the micro-climates of various tree coverage and ideal micro-topography scenarios. The green space in the simulation was designed to be located in the upwind direction, and the open space was located in the downwind direction. Under this scenario, the cooling effects of the green space were transferred to the open space via moving air. However, in reality, changes to wind speed and direction cause air masses to interchange across landscape patches with high frequency, modifying the thermodynamic properties of air masses in complex ways. Also, we only simulated a few sub-scenarios of micro-topographic change due to computational resource constraints. The number of scenarios in the current study is insufficient to create a relationship of cooling impact and distance from green space. Further studies are needed to examine whether there is a linear or non-linear relationship between hill's height and slope and its cooling effects on adjacent built-up areas. In the future investigations, we will build more precise scenarios for surface topography fluctuation. In addition, we will focus on changes in thermal environment in different urban functional zones, and more realistic scenarios with more accurate modeling of buildings and plants will be used. Pollutant dispersion should also be considered in future studies, to ensure that changes to micro-topography will not enhance air contamination. We expect to finally form a function that can be used to estimate cooling effect.

5. Conclusions

This study investigated how tree coverage and micro-topography influence the cooling effects within and beyond a green space during a hot summer day. An ideal landscape that was composed of a green space lying on the windward side and an open space on the leeward side was designed in ENVI-met model. Scenarios with different tree coverage characterized by canopy size and tree number, and different micro-topography (including slope length and slope angle sub-scenarios) were developed to explore the cooling effects of a specific green space.

Our study demonstrated that both canopy size and tree number are important factors characterizing the thermal environment within and beyond the green space during the daytime. However, the cooling effects of these tree coverage sub-scenarios decreased, and even disappeared, at night. The cooling capacity of the green space during the daytime was linearly correlated with the total leaf area of trees. An increase of 1000 m^2 represents a 0.05 ℃ reduction in air temperature. Trees acted as a thermal insulation layer for the atmosphere beneath their crowns, with trees providing cooling effects during the daytime and non-effect or warming effects at night.

Modifications to Micro-topography had stronger cooling effects on both the green space and the open space with asphalt pavement in contrast to the flat terrain scenario. The strongest cumulative cooling capacity on the open space appeared when the slope angle is 20° However, when the slope angle is larger than 20°, the cooling effect brought by upwind green space decreased at the open space on the leeward side.

The current study provides novel insights on how tree coverage and micro-topography influence the near-surface thermal environment. The results of this study could be used by urban planners and designers in residential areas and parks to improve the outdoor thermal comfort levels of surrounding impervious surfaces.

Declaration of Competing Interest

The authors declare that they have no known competing financial interests or personal relationships that could have appeared to influence the work reported in this paper.

Acknowledgments

This work was supported by the National Natural Science Foundation of China (42171100, 31972951, 31670645, 41801182, 41807502 and 42001210), the National Social Science Fund (17ZDA058), the National Key Research Program of China (2016YFC0502704), Fujian Provincial Department of S&T Project (2021I0041,2021T3058 and 2018T3018), the Strategic Priority Research Program of the Chinese Academy of Sciences (XDA23020502), the Ningbo Municipal Department of Science and Technology (2019C10056), the Xiamen Municipal Department of Science and Technology (3502Z20130037 and 3502Z20142016), the Key Laboratory of Urban Environment and Health of CAS (KLUEH-C-201701), the Key Program of the Chinese Academy of Sciences (KFZDSW-324), and the Youth Innovation Promotion Association CAS (2014267).

Appendix

Table S1.

Table S1
Evaluation of the ENVI-met model in previous studies.

Study area	Longitude	Latitude	Land Use/Land Cover (LULC)	Time	Index of Agreement	RMSE	ENVI-met Version	Author
Phoenix, USA	111.68° W	33.31° N	Residential area -Xeric landscaping	June	0.97	2	V3.1 Beta	Middel et al., 2014
			-Oasis landscaping		0.98	1.81		
			-Mesic landscaping		0.99	1.41		
Phoenix, USA	111.68° W	33.31° N	Mixed LULC	January	0.82	2.45	V3.0	A. Hedquist and Brazel, 2014
				July	0.88	1.75		
			Business district	January	0.75	2.77		
				July	0.78	2		
			Open field	January	0.79	2.64		
				July	0.94	1.46		
Putrajaya, Malaysia	101.41° E	2.55° N	Boulevard	July	0.6	1.82	V3.1 Beta	Qaid and Ossen, 2015
Rome, Italy	12.51° E	41.9° N	University campus	July	0.92	1.3	V3.1	Salata et al., 2017
Singapore	103.91° E	1.31° N	Residential area	Autumn	0.87–0.91	1.11–1.41	V3.1	Roth and Lim, 2017
			Residential area	Winter	0.95–0.97	0.66–0.89		
			Residential area	Summer	0.95–0.98	0.52–0.75		
Guangzhou, China	113.33° E	23.15° N	University campus	August-September	0.97	1.01	V4	Yang et al., 2013
Sao Paulo, Brazil	46.61° W	23.53° S	Densely built-up area	April	0.85	1.61	V4 Preview I	Duarte et al., 2015
Rome, Italy	12.51° E	41.9° N	University campus	February	0.87–0.91	1.89–2.79	V3.0, V4	Salata et al., 2016
Taipei, China	121.53° E	25.05° N	Parking lot	July	0.69	1.62		Lin and Lin, 2016
			Urban park	July	0.82	0.32		
Freiburg, Germany	7.85° E	44.00° N	Residential area	August	0.95	0.66	V4	Lee et al., 2016
Portland, USA	122.72° W	45.57° N	Green space	July	0.92–0.99	0.29–2.12	V4.2	Eckmann et al., 2018
Perugia, Italy	12.38° E	43.11° N	Urban Historical area	June	0.71	1.05	V4	Castaldo et al., 2017
Tianjin, China	117.1° E	39.1° N	High school	October	0.77–0.78	0.90–0.97	V4	Zhang et al., 2017
Thessaloniki, Greece	22.9° E	40.65° N	Densely built-up area	August	0.9	1.85	V4	Tsoka et al., 2017
Wuhan, China	114.28° E	30.58° N	Residential area	Summer	0.91	1.46	V4	Zhang et al., 2018
			Residential area	Winter	0.72	0.97		
Bilbao, Spain	2.93° W	43.26° N	Square	August	0.83–0.94	1.00–2.07	V4	Acero and Arrizabalaga, 2018
Hongkong, China	114.17° E	22.31° N	Densely built-up area	August	0.56	0.63	V4	Morakinyo et al., 2019
Nanjing, China	118.78° E	32.06° N	University campus	July	0.95	1.14		Kong et al., 2016
Colorado, USA	105.08° W	39.7° N	Mixed LULC	June	0.97	1.61	V4	Heris et al., 2020
	105.25° W	40.01° N	Mixed LULC	June	0.97	1.5		

References

Acero, J.A., Arrizabalaga, J., 2018. Evaluating the performance of ENVI-met model in diurnal cycles for different meteorological conditions. Theor. Appl. Climatol. 131 (1), 455–469. https://doi.org/10.1007/s00704-016-1971-y.

Akbari, H., Kolokotsa, D., 2016. Three decades of urban heat islands and mitigation technologies research. Energy Build. 133, 834–842. https://doi.org/10.1016/j.enbuild.2016.09.067.

Ali-Toudert, F., 2005. Dependence of Outdoor Thermal Comfort on Street Design in Hot and Dry Climate. Meteorological Institute, University of Freiurg, Germany.

Battaglia, M.A., Douglas, S., Hennigan, C.J., 2017. Effect of the urban heat island on aerosol pH. Environ. Sci. Technol. 51 (22), 13095–13103. https://doi.org/10.1021/acs.est.7b02786.

Beijing Statistics Bureau, 2019. Beijing Statistical Yearbook 2019. China Statistics Press, Beijing.

Bowler, D.E., Buyung-Ali, L., Knight, T.M., Pullin, A.S., 2010. Urban greening to cool towns and cities: a systematic review of the empirical evidence. Landsc. Urban Plan. 97, 147–155. https://doi.org/10.1016/j.landurbplan.2010.05.006.

Caird, M.A., Richards, J.H., Donovan, L.A., 2007. Nighttime stomatal conductance and transpiration in C3 and C4 plants. Plant Physiol. 143 (1), 4–10. https://doi.org/10.1104/pp.106.092940.

Castaldo, V.L., Pisello, A.L., Pigliautile, I., Piselli, C., Cotana, F., 2017. Microclimate and air quality investigation in historic hilly urban areas: experimental and numerical investigation in central Italy. Sust. Cities Soc. 33, 27–44. https://doi.org/10.1016/j.scs.2017.05.017.

Ding, F., Pang, H., Guo, W., 2018. Impact of the urban heat island on residents' energy consumption: a case study of Qingdao. IOP Conf. Ser. Earth Environ. Sci. 121 (3), 032026 https://doi.org/10.1088/1755-1315/121/3/032026.

Duarte, D.H.S., Shinzato, P., Gusson, C.d.S., Alves, C.A., 2015. The impact of vegetation on urban microclimate to counterbalance built density in a subtropical changing climate. Urban Clim. 2, 224–239. https://doi.org/10.1016/j.uclim.2015.09.006, 14, Part.

Eckmann, T., Morach, A., Hamilton, M., Walker, J., Simpson, L., Lower, S., McNamee, A., Haripriyan, A., Castillo, D., Grandy, S., Kessi, A., 2018. Measuring and modeling microclimate impacts of Sequoiadendron giganteum. Sust. Cities Soc. 38, 509–525. https://doi.org/10.1016/j.scs.2017.12.028.

Emmanuel, R., Loconsole, A., 2015. Green infrastructure as an adaptation approach to tackling urbanoverheating in the Glasgow Clyde Valley Region, UK. Landsc. Urban Plan. 138, 71–86. https://doi.org/10.1016/j.landurbplan.2015.02.012.

Ge, F., Zhang, L., Wang, J., Tian, G., Feng, Y., 2016. Multi-scale temporal charachteristics and periodic analysis of urban heat island - a case study of Beijing. Journal of Beijing Normal University (Natural Science), 52(2): 210–215 (in Chinese with English Abstract). 10.16360/j.cnki.jbnuns.2016.02.017.

Ghaffarianhoseini, A., Berardi, U., Ghaffarianhoseini, A., 2015. Thermal performance characteristics of unshaded courtyards in hot and humid climates. Build. Environ. 87, 154–168. https://doi.org/10.1016/j.buildenv.2015.02.001.

Hamada, S., Ohta, T., 2010. Seasonal variations in the cooling effect of urban green areas on surrounding urban areas. Urban For. Urban Green. 9 (1), 15–24. https://doi.org/10.1016/j.ufug.2009.10.002.

Hamada, S., Tanaka, T., Ohta, T., 2013. Impacts of land use and topography on the cooling effect of green areas on surrounding urban areas. Urban For. Urban Green. 12, 426–434. https://doi.org/10.1016/j.ufug.2013.06.008.

Hedquist, B., Brazel, A.J., 2014. Seasonal variability of temperatures and outdoor human comfort in Phoenix, Arizona, U.S.A. Build. Environ. 72, 377–388. https://doi.org/10.1016/j.buildenv.2013.11.018.

Herath, H.M.P.I.K., Halwatura, R.U., Jayasinghe, G.Y., 2018. Evaluation of green infrastructure effects on tropical Sri Lankan urban context as an urban heat island adaptation strategy. Urban For. Urban Green. 29, 212–222. https://doi.org/10.1016/j.ufug.2017.11.013.

Heris, M.P., Middel, A., Muller, B., 2020. Impacts of form and design policies on urban microclimate: assessment of zoning and design guideline choices in Urban

redevelopment projects. Landsc. Urban Plan. 202, 103870 https://doi.org/10.1016/j.landurbplan.2020.103870.
Jauregui, E., 1990. Influence of a large urban park on temperature and convective precipitation in a tropical city. Energy Build. 15 (3), 457–463. https://doi.org/10.1016/0378-7788(90)90021-A.
Jonckheere, I., Fleck, S., Nackaerts, K., Muys, B., Coppin, P., Weiss, M., Baret, F., 2004. Review of methods for in situ leaf area index determination Part I. Theories, sensors and hemispherical photography. Agric. For. Meteorol. 121, 19–35. https://doi.org/10.1016/j.agrformet.2003.08.027.
Kasten, F., Czeplak, G., 1980. Solar and terrestrial radiation dependent on the amount and type of cloud. Sol. Energy 24 (2), 177–189. https://doi.org/10.1016/0038-092X(80)90391-6.
Kondo, K., Tsuchiya, M., Sanada, S., 2002. Evaluation of effect of micro-topography on design wind velocity. J. Wind Eng. Ind. Aerodyn. 90 (12), 1707–1718. https://doi.org/10.1016/S0167-6105(02)00281-7.
Kong, F., Sun, C., Liu, F., Yin, H., Jiang, F., Pu, Y., Cavan, G., Skelhorn, C., Middel, A., Dronova, I., 2016. Energy saving potential of fragmented green spaces due to their temperature regulating ecosystem services in the summer. Appl. Energy 183, 1428–1440. https://doi.org/10.1016/j.apenergy.2016.09.070.
Kong, F., Yin, H., James, P., Hutyra, L.R., He, H.S., 2014. Effects of spatial pattern of greenspace on urban cooling in a large metropolitan area of eastern China. Landsc. Urban Plan. 128, 35–47. https://doi.org/10.1016/j.landurbplan.2014.04.018.
Lalic, B., Mihailovic, D.T., 2004. An empirical relation describing leaf-area density inside the forest for environmental modelling. J. Appl. Meteorol. Climatol. 43 (4), 641–645. https://doi.org/10.1175/1520-0450(2004)0432.0.CO;2.
Lee, H., Mayer, H., Chen, L., 2016. Contribution of trees and grasslands to the mitigation of human heat stress in a residential district of Freiburg, Southwest Germany. Landsc. Urban Plan. 148, 37–50. https://doi.org/10.1016/j.landurbplan.2015.12.004.
Lin, B.S., Lin, C.T., 2016. Preliminary study of the influence of the spatial arrangement of urban parks on local temperature reduction. Urban For. Urban Green. 20, 348–357. https://doi.org/10.1016/j.ufug.2016.10.003.
Liu, Y., Du, J., Hu, P., Ma, M., Hu, D., 2020. Microtopographic modification conserves urban wetland water quality by increasing the dissolved oxygen in the wet season. J. Environ. Sci. 87, 71–81. https://doi.org/10.1016/j.jes.2019.06.003.
Meehl, G.A., Tebaldi, C., 2004. More intense, more frequent, and longer lasting heat waves in the 21st century. Science 305, 994–997. https://doi.org/10.1126/science.1098704.
Merckx, T., Souffrea, C., Kaiser, A., Baardsen, L.F., Backeljau, T., Bonte, D., Brans, K.I., Cours, M., Dahirel, M., Debortoli, N., De Wolf, K., Engelen, J.M.T., Fontaneto, D., Gianuca, A.T., Govaert, L., Hendrickx, F., Higuti, J., Lens, L., Martens, K., Matheve, H., Matthysen, E., Piano, E., Sablon, R., Schön, I., Van Doninck, K., De Meester, L., Van Dyck, H., 2018. Body-size shifts in aquatic and terrestrial urban communities. Nature 558 (7708), 113–116. https://doi.org/10.1038/s41586-018-0140-0.
Middel, A., Häb, K., Brazel, A.J., Martin, C.A., Guhathakurta, S., 2014. Impact of urban form and design on mid-afternoon microclimate in Phoenix Local Climate Zones. Landsc. Urban Plan. 122, 16–28. https://doi.org/10.1016/j.landurbplan.2013.11.004.
Morakinyo, T.E., Lai, A., Lau, K.K.L., Ng, E., 2019. Thermal benefits of vertical greening in a high-density city: case study of Hong Kong. Urban For. Urban Green. 37, 42–55. https://doi.org/10.1016/j.ufug.2017.11.010.
Myint, S., Wentz, E., Brazel, A., Quattrochi, D., 2013. The impact of distinct anthropogenic and vegetation features on urban warming. Landsc. Ecol. 28 (5), 959–978. https://doi.org/10.1007/s10980-013-9868-y.
Nowak, D.J., McHale, P., Ibarra, M., Crane, D., Stevens, J.C., Luley, C., 1998. Modeling the effects of Urban vegetation on air pollution. In: Gryning, S.E., Chaumerliac, N. (Eds.), Air Pollution Modeling and its Application XII. Springer US, Boston, MA, pp. 399–407.
Patz, J.A., Campbell-Lendrum, D., Holloway, T., Foley, J.A., 2005. Impact of regional climate change on human health. Nature 438 (7066), 310–317. https://doi.org/10.1038/nature04188.
Pfister, L., Sigmund, A., Olesch, J., Thomas, C.K., 2017. Nocturnal near-surface temperature, but not flow dynamics, can be predicted by microtopography in a mid-range mountain valley. Bound. Layer Meteorol. 165 (2), 333–348. https://doi.org/10.1007/s10546-017-0281-y.
Potchter, O., Cohen, P., Bitan, A., 2006. Climatic behavior of various urban parks during hot and humid summer in the mediterranean city of Tel Aviv, Israel. Int. J. Climatol. 26 (12), 1695–1711. https://doi.org/10.1002/joc.1330.
Qaid, A., Ossen, D.R., 2015. Effect of asymmetrical street aspect ratios on microclimates in hot, humid regions. Int. J. Biometeorol. 59, 657–677. https://doi.org/10.1007/s00484-014-0878-5.
Roth, M., Lim, V.H., 2017. Evaluation of canopy-layer air and mean radiant temperature simulations by a microclimate model over a tropical residential neighbourhood. Build. Environ. 112, 177–189. https://doi.org/10.1016/j.buildenv.2016.11.026.
Salata, F., Golasi, I., de Lieto Vollaro, R., de Lieto Vollaro, A., 2016. Urban microclimate and outdoor thermal comfort. A proper procedure to fit ENVI-met simulation outputs to experimental data. Sust. Cities and Soc. 26, 318–343. https://doi.org/10.1016/j.scs.2016.07.005.
Salata, F., et al., 2017. Relating microclimate, human thermal comfort and health during heat waves: an analysis of heat island mitigation strategies through a case study in an urban outdoor environment. Sust. Cities Soc. 30, 79–96. https://doi.org/10.1016/j.scs.2017.01.006.
Shashua-Bara, L., Hoffman, M.E., 2000. Vegetation as a climatic component in the design of an urban street an empirical model for predicting the cooling effect of urban green areas with trees. Energy Build. 31, 221–235. https://doi.org/10.1016/S0378-7788(99)00018-3.
Simon, H., 2016. Modeling Urban microclimate: Development, Implementation and Evaluation of New and Improved Calculation Methods for the Urban Microclimate Model ENVI-met. Doctor of Philosophy. Department of Chemistry, Pharmacy and Geosciences. Johannes Gutenberg University Mainz, Germany.
Simon, H., Lindén, J., Hoffmann, D., Braun, P., Bruse, M., Espera, J., 2018. Modeling transpiration and leaf temperature of urban trees – a case study evaluating the microclimate model ENVI-met against measurement data. Landsc. Urban Plan. 174, 33–40. https://doi.org/10.1016/j.landurbplan.2018.03.003.
Smardon, R.C., 1988. Perception and aesthetics of the urban environment: review of the role of vegetation. Landsc. Urban Plan. 15 (1), 85–106. https://doi.org/10.1016/0169-2046(88)90018-7.
Sodoudi, S., Zhang, H., Chi, X., Müller, F., Li, H., 2018. The influence of spatial configuration of green areas on microclimate and thermal comfort. Urban For. Urban Green. 34, 85–96. https://doi.org/10.1016/j.ufug.2018.06.002.
Tejima, M., 1995. Effects of roughness parameter due to buildings and thermal property of construction materials on temperature distribution in a housing complex. Geogr. Sci. 50 (2), 91–102. https://doi.org/10.20630/chirikagaku.50.2_91.
Thom, J.K., Coutts, A.M., Broadbent, A.M., Tapper, N.J., 2016. The influence of increasing tree cover on mean radiant temperature across a mixed development suburb in Adelaide, Australia. Urban For. Urban Green. 20 (Supplement C), 233–242. https://doi.org/10.1016/j.ufug.2016.08.016.
Tsoka, S., Tsikaloudaki, K., Theodosiou, T., 2017. Urban space's morphology and microclimatic analysis: a study for a typical urban district in the Mediterranean city of Thessaloniki, Greece. Energy Build. 156, 96–108. https://doi.org/10.1016/j.enbuild.2017.09.066.
Vanos, J.K., Middel, A., McKercher, G.R., Kuras, E.R., Ruddell, B.L., 2016. Hot playgrounds and children's health: a multiscale analysis of surface temperatures in Arizona, USA. Landsc. Urban Plan. 146, 29–42. https://doi.org/10.1016/j.landurbplan.2015.10.007.
Vaz Monteiro, M., Doick, K.J., Handley, P., Peace, A., 2016. The impact of greenspace size on the extent of local nocturnal air temperature cooling in London. Urban For. Urban Green. 16, 160–169. https://doi.org/10.1016/j.ufug.2016.02.008.
Wang, W., Zhang, W., Cai, X., 2009. Variation of temperature and precipitation in Beijing during last 50 years. J. Arid Meteorol., 27 (4), 350–354. https://doi.org/10.3969/j.issn.1006-7639.2009.04.009 (in Chinese with English Abstract).
Wang, Y., Shen, J., Xiang, W., 2018. Ecosystem service of green infrastructure for adaptation to urban growth: function and configuration. Ecosyst. Health Sustain. 4 (5), 132–143. https://doi.org/10.1080/20964129.2018.1474721.
Wong, L.P., Alias, H., Aghamohammadi, N., Aghazadeh, S., Nik Sulaiman, N.M., 2017. Urban heat island experience, control measures and health impact: a survey among working community in the city of Kuala Lumpur. Sust. Cities Soc. 35, 660–668. https://doi.org/10.1080/10.1016/j.scs.2017.09.026.
Wu, Z., Chen, L., 2017. Optimizing the spatial arrangement of trees in residential neighborhoods for better cooling effects: integrating modeling with in-situ measurements. Landsc. Urban Plan. 167, 463–472. https://doi.org/10.1016/j.landurbplan.2017.07.015.
Yadav, N., Sharma, C., Peshin, S.K., Masiwal, R., 2017. Study of intra-city urban heat island intensity and its influence on atmospheric chemistry and energy consumption in Delhi. Sust. Cities Soc. 32, 202–211. https://doi.org/10.1016/j.scs.2017.04.003.
Yang, X., Zhao, L., Bruse, M., Meng, Q., 2013. Evaluation of a microclimate model for predicting the thermal behavior of different ground surfaces. Build. Environ. 60, 93–104. https://doi.org/10.1016/j.buildenv.2012.11.008.
Zhang, A., et al., 2017. An integrated school and schoolyard design method for summer thermal comfort and energy efficiency in Northern China. Build. Environ. 124, 369–387. https://doi.org/10.1016/j.buildenv.2017.08.024.
Zhang, L., Zhan, Q., Lan, Y., 2018. Effects of the tree distribution and species on outdoor environment conditions in a hot summer and cold winter zone: a case study in Wuhan residential quarters. Build. Environ. 130, 27–39. https://doi.org/10.1016/j.buildenv.2017.12.014.
Zhao, J., 2010. Species Composition and Spaital Distribution of Urban Plants Within the Built-Up Areas of Beijing, China. Doctor of Philosophy. Research Center of Eco-Environmental Sciences. University of Chinese Academy of Sciences, China (in Chinese with English abstract).
Zheng, Z., Ren, G., Wang, H., Dou, J., Gao, Z., Duan, C., Li, Y., Ngarukiyimana, J.P., Zhao, C., Cao, C., Jiang, M., Yang, Y., 2018. Relationship between fine-particle pollution and the urban heat island in beijing, china: observational evidence. Bound. Layer Meteorol. 169 (1), 93–113. https://doi.org/10.1007/s10546-018-0362-6.
Zölch, T., Rahman, M.A., Pfleiderer, E., Wagner, G., Pauleit, S., 2019. Designing public squares with green infrastructure to optimize human thermal comfort. Build. Environ. 149, 640–654. https://doi.org/10.1016/j.buildenv.2018.12.051.